AD-A193 767 ADVANCED PROCESSING AND PROPERTIES OF HIGH PERFORMANCE ALLOYS(U) PENNSYLVANIA STATE UNIV UNIVERSITY PARK DEPT OF MATERIALS SCIENCE AND ENGINEE RING D A KOSS MAR 88 1/1

UNCLASSIFIED N00014-86-K-0381 F/G 11/6.2 NL

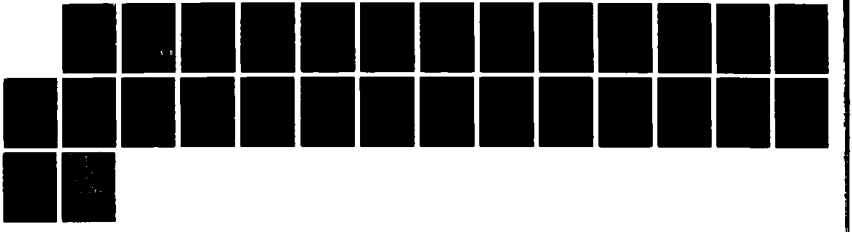

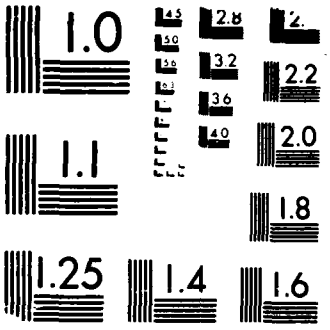

TECHNICAL REPORT NO. 9

TO

The Office of Naval Research
Contract No. NOOO14-86-K-0381

ADVANCED PROCESSING AND PROPERTIES OF HIGH PERFORMANCE ALLOYS

D. A. Koss

Department of Materials Science and Engineering
The Pennsylvania State University
University Park, PA 16802

Report for the period 1 February 1987 - 31 December 1987

SECURITY CLASSIFICATION OF THIS PAGE (When Data Entered)

REPORT DOCUMENTATION PAGE		READ INSTRUCTIONS BEFORE COMPLETING FORM
1. REPORT NUMBER Technical Report No. 9	2. GOVT ACCESSION NO.	3. RECIPIENT'S CATALOG NUMBER
4. TITLE (and Subtitle) Advanced Processing and Properties of High Performance Alloys		5. TYPE OF REPORT & PERIOD COVERED 6. PERFORMING ORG. REPORT NUMBER
7. AUTHOR(s) D. A. Koss		8. CONTRACT OR GRANT NUMBER(s) N00014-86-K-0381
9. PERFORMING ORGANIZATION NAME AND ADDRESS Department of Materials Science and Engineering The Pennsylvania State University University Park, PA 16802		10. PROGRAM ELEMENT, PROJECT, TASK AREA & WORK UNIT NUMBERS
11. CONTROLLING OFFICE NAME AND ADDRESS Office of Naval Research 800 N. Quincy St. Arlington, VA 22217		12. REPORT DATE March 1988 13. NUMBER OF PAGES 26
14. MONITORING AGENCY NAME & ADDRESS(if different from Controlling Office)		15. SECURITY CLASS. (of this report) 15a. DECLASSIFICATION/DOWNGRADING SCHEDULE

16. DISTRIBUTION STATEMENT (of this Report)

Distribution of this document is unlimited.

17. DISTRIBUTION STATEMENT (of the abstract entered in Block 20, if different from Report)

18. SUPPLEMENTARY NOTES

19. KEY WORDS (Continue on reverse side if necessary and identify by block number)

Processing, Fracture mechanisms, Void/Pore linking, low cycle fatigue, ~~Cu-Nb~~ alloys

20. ABSTRACT (Continue on reverse side if necessary and identify by block number)

Progress is reviewed for a research program whose purpose is to establish a broad-based understanding of the application and consequences of advanced processing techniques, especially as they influence the strength and fracture resistance of high performance structural alloys. While some of the research is specific to certain alloy systems, much of the program constitutes a fundamental study of the deformation and fracture of engineering alloys containing processing-induced defects. Progress for the period February 1, 1987 to December 31, 1987, is reviewed for the following projects within the program:

DD FORM 1 JAN 73 1473 EDITION OF 1 NOV 65 IS OBSOLETE

SECURITY CLASSIFICATION OF THIS PAGE (When Data Entered)

20. Con't.

(1) the mechanism of strain-induced void/pore linking during ductile fracture,

(2) the influence of porosity on low cycle fatigue, and

(3) the processing and properties of Cu-Nb microcomposites.

ADVANCED PROCESSING AND PROPERTIES OF HIGH PERFORMANCE ALLOYS

INTRODUCTION

The next generation of advanced structural systems will require high performance materials which exhibit dramatic improvements in both strength and fracture resistance over a wide range of temperatures and environments. The development of such materials is becoming increasingly dependent on advanced processing techniques. For example, the application of rapid solidification processing has been used to develop new families of high performance alloys in powder or flake form, which in turn require additional processing (usually by powder metallurgy techniques) to achieve fully dense components.[1-4]

A fundamental problem in advanced alloy technology is that the rate of application of new processing methods exceeds the basic knowledge base necessary to anticipate fully the resulting behavior of the component in service. Thus, while novel alloy microstructures are created through advanced processing techniques, the promise of improved properties is usually accompanied by the potential for a new set of problems. For example, rapidly solidified dispersion hardened alloys may exhibit superior short time tensile strengths but inadequate high temperature creep strength due to the stabilization of fine grain sizes and the resulting enhanced grain boundary sliding. As a result, despite some notable improvements in material's properties, in-service reliability may be impaired.

The primary purpose of the present research is to provide a broad-based understanding of the applications and consequences of certain advanced processing techniques when used to create new high performance alloys. The research ranges in scope from fundamental studies of the mechanisms of void or pore linking during ductile fracture and low cycle fatigue to the processing-property relationships in Cu-Nb microcomposites. The present report summarizes progress in the areas of research for the period 1/31/87 to 12/31/87 performed under the auspices of Contract No. NOOO14-86-K-0381. The research areas are as follows:

(1) the mechanism of strain-induced void/pore linking during ductile fracture,

(2) the influence of porosity on low cycle fatigue, and

(3) processing and properties of Cu-Nb microcomposites.

A significant impact of the above research is the educational experience derived by the graduate students involved. The following students have been a part of this ONR program during the period cited: Paul Magnusen, Ph.D., June 1987; Dale Gerard, Ph.D. candidate; Kevin Zeik, Ph.D. candidate; and Andrew Geltmacher, M.S. candidate.

SUMMARY OF RESEARCH

1. The Mechanism of Strain-Induced Void/Pore Linking During Ductile Fracture[with Paul Magnusen, Ph.D., June 1987, Andrew Geltmacher, M.S. candidate, Prof. David Srolovitz, Univ. of Michigan and Prof. Jong Lee, Michigan Technological University]

That the presence of pre-existing porosity and the subsequent pore linking during deformation strongly affects ductile fracture is well known (see for example, Ref. 5). It is also well established that void linking is an important stage of the ductile fracture process. Despite its importance, the mechanism of strain-induced void/pore linking is only now beginning to be understood as a result of our studies.[6-9] This situation developed because nearly all theoretical analyses of low temperature fracture based on void/pore growth and linking assumed regular arrays of holes or cavities[10-18] as well as arbitrary, geometrically based void linking criteria.[19-21] Relying on the modeling of three-dimensional void/pore arrays by two-dimensional distributions of holes, we have been studying the void linking process that occurs during low temperature ductile fracture. The program has been based on using both experiments and computer simulation to examine the fracture process of specimens containing arrays of holes. The hole arrays are subject to constraints imposed on (a) the area fraction, (b) the hole size, and (c) the minimum spacing between holes; in the latter case, the degree of hole clustering may be controlled. The behavior of specimens containing both random and regular arrays of holes has been examined. An important aspect of the program has been its reliance on the complementing efforts of both experimental studies and computer simulation, using each to guide the other.

The experimental studies indicate that increasing minimum hole spacing, which decreases the degree of hole clustering, increases both strength and ductility.[6-8] The results also indicate that specimens containing random arrays of holes are less ductile than their regular array counterparts (at the same hole size and area fraction). This effect is illustrated in Fig. 1, and, as seen, depends on the degree to which clustering occurs in the array (increasing minimum hole spacing decreases clustering). Other results show that the magnitude of the ductility differences between uniformly spaced and clustered hole arrays depends also on the strain hardening. These data clearly indicate the importance of the random nature of void/pore distributions in controlling ductile fracture. Specifically, models of ductile fracture based on regular arrays of voids or holes[10-18] are inherently limited by their reliance on both an unrealistic distribution and an arbitrary void linking criterion.[19-21] For example, a void/hole linking criterion which provides a reasonable failure strain for one material will very likely be incorrect for another material with differing strain hardening behavior or a different void/pore distribution.

The observed effects of hole distributions on ductile fracture may be readily understood in terms of a physical model recently proposed for void linking during ductile, microvoid fracture.[6-7] In that model, the fracture process is a consequence of a multi-stage sequence. In the first stage, local strain gradients develop near individual holes/pores at small macroscopic strains. Secondly, increasing macroscopic strain localizes strain and triggers flow instabilities and ligament fracture between closely spaced and favorably oriented holes/voids. During the third stage, failure of the ligament between holes occurs, and an elongated hole is created which, due to its eccentric shape and size, tends to further localize flow along its major axis.

Once elongated holes/voids are created by initial linking, a Fourth Stage results from the statistical location of the adjacent holes. If an adjacent hole/void is favorablly located such that intense deformation across that ligament will cause it to fail and then link to the previously linked pair of of holes/voids (which connected in the previous Stage). Stages 3

and 4 essentially repeat with the statistics now relating to the location of a fourth hole to the expanded plastic zone of the linked triplet. If a third hole is not favorably located, then macroscopic deformation proceeds until another pair of holes links and Stage Four of the process repeats. As deformation continues, hole linking results in increased plastic zone sizes which in turn increase the probability of successive holes/voids being linked. Thus the early Stages of void/hole linking occur via localized flow concentration, instability, and /or ligament fracture, and eventually percolation .

As deformation continues but with only a few additional percent of the load-bearing cross section area removed by hole/void linking, the final Stage of failure is triggered: an imperfection-initiated general instability [22-23] or the propagation of a crack-like defect. In this Fifth Stage, a sufficient number of voids/holes have linked to create an imperfection or crack-like defect whose severity increases with strain as the holes link. This triggers a macroscopic shear instability across the remaining cross sectional area of the specimen, causing failure by the void sheet mechanism between large voids.

The step-wise process of void linking at low temperatures has also been simulated by a computer model. Given the importance of local plasticity near holes/voids in the process, the simulation relies on experimental data which have been obtained in order to describe the local plasticity near (a) isolated single holes, (b) pairs of unlike holes, (c) pairs of linked holes, and (d) by extension of (c), multiple holes which have linked. Detailed measurements of the development of local strain gradients in a tensile strain field have been made in 1100 Al and brass sheets.[24] These data have in turn been fit to empirical equations, similar in form to those which describe the elastic stress fields near holes, which describe the localized thickness strain component in terms of hole parameters and macroscopic strains. In addition to the local, near-hole strain distributions, the simulation relies on a criterion for the failure of the ligament between holes; in our study, a thickness strain criterion was observed to control ligament failure.[7,8] It is important to note that the

simulation uses no adjustable parameters other than those experimentally based ones which describe the plasticity near holes and the failure criterion for hole linking.

The simulated sequence of fracture events resulting in failure of specimens containing various hole arrays has been examined for the hole plasticity/linking conditions obtained by experiment on 1100 Al and brass. An example of the simulation results for the Al is shown in Fig. 2. The hole/void linking sequence previously described is evident: (a) local strain development near individual holes, (b) flow localization and ligament failure between closely spaced favorably oriented holes, (c) strain amplification due to linking and subsequently additional linking if other holes are favorably located, and (d) a general instability as linking is percolated across the specimen.

An example of the agreement between the computer simulation and experimental data is shown in Fig. 3. In this case, the effect of increasing the minimum hole spacing (increasing the uniformity of hole spacing) on ductility is shown for a given area fraction and hole diameter. The computer simulation accurately predicts the experimentally determined increase in ductility with increasing minimum hole spacing, especially in view of the absence of adjustable parameters which may be used to force a fit. Similar agreement is obtained for the less ductile, lower strain-hardening aluminum.

Based on our progress in identifying and modeling the basic void linking process, current research is extending that base to include other effects of void "microstructures," such as those in containing a range of hole size distributions and shapes. For example, the tensile behavior of specimens containing distributions of circular holes of (a) two different sizes (bimodal distribution) and (b) a spectrum of different sizes is being examined. Initial efforts are concentrating on prediction of fracture behavior based on computer simulation. Subsequently, experimental data with specific hole size distributions will be obtained as a means of testing the predictions of the simulations and as a basis for refining that analysis. The effects of materials flow characteristics are being evaluated by both computer

simulation and the experimental testing materials with two different strain hardening capacities (1100 Al and 70-30 brass).

2. The Influence of Porosity on Low Cycle Fatigue (with Dale Gerard, Ph.D. candidate)

Numerous investigations have examined the deleterious effects of porosity on uniaxial tension and high cycle fatigue behavior; for example see Ref. 1 The reductions in high cycle fatigue life of porous specimens have been attributed to local stress concentrations near pores which result in localized slip even though the nominal stress remains in the elastic regime. Although there has been many studies which investigate the effects of porosity on high cycle fatigue behavior, there have been no fundamental studies examining the effects of porosity on low cycle fatigue behavior. This is significant since the resistance of materials to low cycle fatigue failure, wherein the material is fully plastic, is often quite different than the response to high cycle fatigue when the peak stress is in the elastic regime. The purpose of this investigation is to examine the influence of porosity on low cycle fatigue behavior. Powder-processed titanium containing various levels of porosity is being used as a model material. Although this study is based on powder-processed materials, the results should also apply to cast materials which frequently have residual porosity, or to those alloy/composite systems which readily form voids at small strains due to poor interfacial bonding.

(a) Experimental Behavior

Commercially pure titanium specimens containing several levels of porosity have been prepared using conventional powder processing techniques. These specimens vary in pore volume fraction (0.5 to 6%) and pore size (25 and 60μm at 6% porosity and 20 to 30μm at the all other porosity levels). In all cases, the pores have well rounded shapes.

Axial cylindrical push-pull (fully reversed) low cycle fatigue have been performed under total strain control at amplitudes of 0.75 and 1.5% strain and at frequencies of 0.25 and 0.15 Hz respectively. During the tests the following parameters were monitored: (a)

the cyclic stress-strain behavior was determined by continuously recording the peak stress, and selectively measuring stress-strain hystersis loops, (b) the number of cycles for microcrack initiation, as well as the growth and link-up stage, was obtained by interrupting tests and making surface replicas, (c) crack closure effects were observed, and (d) the number of cycles to failure was also recorded.

Large reductions in low cycle fatigue life are observed at both of the strain amplitudes examined for all porosity levels and pore sizes. Fig. 4 demonstrates that low cycle fatigue life deteriorates rapidly with increasing pore volume fraction, the effect being more pronounced at large pore sizes. Even the presence of 0.5 vol % porosity causes more than a 50% loss in fatigue life. The loss of fatigue life due to porosity is also more severe at high strain amplitudes.

In order to analyze the fundamental causes for the reductions in low cycle fatigue life, it is useful to separate low cycle fatigue into a sequence of three stages: microcrack initiation, microcrack growth and linking, and macrocrack propagation. Acceleration of any of these failure stages will result in a deterioration in low cycle fatigue properties. In the present study, specimens were carefully examined to determine the number of cycles (a) to initiate a 15μm long microcrack, and (b) from the onset of macrocrack propagation to failure, and (c) given the data for (a) and (b), for microcrack growth and linking. [Note that macrocrack propagation is defined as commencing when a 5% reduction in the specimen compliance is measured.] Fig. 5 illustrates that each of the fatigue failure stages accelerate with increasing porosity level, pore size, and strain amplitude. The acceleration is especially large for microcrack initiation, although each of the stages is accelerated by the presence of porosity.

The reduction in low cycle fatigue life due to the microcrack initiation is a result of the strain concentrations which are generated near pores on the specimen surface. The data in Fig. 5a show that once pores are present the number of cycles to initiate a 15μm microcrack is essentially independent of the porosity level. For a given porosity level this figure also

indicates that microcrack initiation accelerates with increasing strain amplitude and pore size. The latter effect may be related to the interconnected nature of the 6% coarse porosity material; this problem is being investigated. A theoretical analysis is also being developed which estimates the number of cycles to initiate crack: this model is discussed and compared with experimental results in the constitutive modeling section.

The next failure stage, which is very complex, consists of microcrack growth and microcrack linking which occur concurrently. Microcrack growth commences once a crack initiates. The microcrack growth rate will vary not only with changes in crack length, but also when the crack encounters grain boundaries, pores, or when linking occurs with other cracks. In Fig. 6, the short crack (i.e. microcrack) growth rates, da/dN, of the fully dense and 6% fine porosity level specimens are shown for specimens tested at total strain amplitudes of 1.5%. Since linear elastic fracture mechanics are not valid for fully plastic deformation, the crack growth data has been obtained by using a method developed by Dowling which incorporates the J integral.[25] The solid lines in each figure indicate extrapolated values of large crack growth regime obtained by Beevers et al.[26] for fully dense titanium. In both the fully dense and 6% porous specimens, the short crack growth rates are higher than that of the large cracks. This is not surprising since such crack growth behavior has been observed in many investigations, for example, see Ref. 4. However, what is surprising is that the short crack growth rate is not strongly affected by porosity; see Fig. 6 (note: similar behavior is also observed at 0.75% total strain amplitude). Only temporary increases in short crack growth rates are observed and these occur when cracks approach pores or other cracks. The lack of an effect of porosity on short crack growth behavior is a significant result since to our knowledge no other investigators have examined the effects of porosity on short crack growth during low cycle fatigue testing.

Another significant observation is that, unlike in high cycle fatigue where short crack growth is frequently observed to arrest at or near grain boundaries, the short cracks were rarely observed to arrest at grain boundaries in low cycle fatigue. This is undoubtedly a

result of the larger driving forces for crack growth associated with low cycle (fully plastic) fatigue deformation.

In view of the relatively small effects of porosity on short crack growth, the effect of porosity on the combination of microcrack growth and linking (Fig. 5) must be in the linking stage. Quantitative measurements of microcrack densities, average crack size and orientation as a function of cycles are currently in progress. Qualitative observations strongly suggest that the high density of short cracks which initiate at high porosity levels result in accelerated linking and thereby a decrease in the number of cycles to reach macrocrack proportions.

Macrocrack growth has been arbitrarily defined as commencing when a five percent reduction in compliance is measured. The abrupt changes in compliance as well as its derivative which result from the onset of macrocrack propagation permit an accurate determination of the number of cycles to the onset of macrocrack growth.

The experimental data show that macrocrack life decreases slightly with increasing strain amplitude and is somewhat accelerated by increases in porosity level and size; see Fig. 5c. Fractography also indicates that the macrocrack fracture paths are much more tortuous (increasing in tortuosity with increasing porosity level) than the fracture paths of the fully dense material which exhibits a relatively flat, planar failure path normal to the fatigue axis. Thus, although the macrocrack growth of a porous specimen is accelerated by a factor of 2 to 4 for each of the porosity conditions examined, the cracks in the porous specimens actually travel larger distances due to the irregularity of the failure path. Therefore, the macrocrack growth along the local crack path in the porous specimens must be occurring at significantly faster rates than those in the fully dense materials.

Previous investigators[27-29] have observed small or even no effect of porosity on growth rates of long cracks in high cycle fatigue once the size of the crack-tip plastic zone approaches the average pore spacing. These investigators have generally concluded that porosity causes only minimal increases in high cycle fatigue crack growth rates because of

(1) the increased length of the crack path as a result of crack deflection, and (2) the associated increase in roughness-induced crack closure. Measurements of the opening and closure loads for both short and long cracks as a function of porosity are currently being performed. Preliminary data for the 0.5% porous material indicate that long cracks open at slightly compressive stresses and that crack closure occurs at highly compressive stresses at 0.75% total strain amplitude testing. These results are in agreement with data for steel also in fully reversed plastic strain cycling.[30] Once closure measurements have been completed, the effect of porosity on crack growth can be analyzed in terms of both crack closure effects and crack deflection.

(b) Constitutive Modeling

The final goal of this project is to develop a constitutive equation which predicts the effect of porosity on the low cycle fatigue life in terms of the intrinsic cyclic material parameters. In order to develop an equation which accurately predicts the low cyclic fatigue life of a porous material, a theoretical analysis is being developed to predict the number of cycles (a) to initiate a 15μm crack, (b) to propagate and link microcracks, and (c) to propagate the macrocrack to failure.

The estimation of the number of cycles necessary to initiate a 15μm long crack from a pore may be separated into three aspects:

(1) Experimentally measured plastic strain distributions near holes[24] are used in conjunction with a stress/strain concentration theory[31] to theoretically estimate the plastic strain profiles which form adjacent to a pore in a fully plastic matrix. The theory predicts local plastic strain distributions ε_{local} terms of the elastic stress concedntration factor K_T, the nominal strain ε_n, and the strsain hardening exponent n such that

$$\varepsilon_{local} = \left[K_T^2 \, \varepsilon_n^{n+1} \left(\frac{A_{nom}}{A_{net}} \right)^{\left(\frac{1-n}{n}\right)} \right]^{-(n+1)}$$

holes such as is shown in Fig. 7. As seen, there is good agreement between theory and experiment for the case of a circular hole.

From the modeling of the pore in two dimensions as through-thickness hole, theoretical strain profiles have been calculated at the peak tensile strain of each cycle on the plane of maximum strain as a function of distance from the pore. These profiles are estimates of the strain distributions adjacent to an isolated pore of elliptical shape in a material which has a strain hardening capacity. Since the local strain amplitudes near the holes (pores) can be determined as a function of cycles and distance from the pore, they can be incorporated into a plastic strain-life analysis to predict local failure (crack initiation).

(2) Next, the theoretical plastic strain amplitude profiles generated after each cycle are used to estimate the number of cycles to failure for the materials in the region adjacent to the pore. The failure estimates are made based on local strain amplitudes at predetermined distance(s) from the hole which correspond to microcrack lengths. The failure predictions are based on the Coffin-Manson strain-life behavior of fully dense titanium.

(3) Finally, cumulative damage theory is used to estimate the number of cycles to initiate a crack by incorporating the low cycle fatigue failure predictions of the material adjacent to the pore after each cycle.

More theoretical work needs to be completed in the microcrack initiation facet of the program, but the initial results are encouraging. For example, using the above analysis, we have theoretically predicted the number of cycles to initiate cracks in specimens tested at 1.5% and 0.75% total strain amplitudes and containing a range of porosity contents. Fig. 8 shows that except for the case of 6% fine porosity, agreement between theory and experiment is excellent.

The remainder of the constitutive model for predicting the number of cycles for each of the remaining low cycle fatigue failure stages must incorporate the effects of short crack growth, microcrack link-up, the interactions between the two mechanisms, and macrocrack propagation. Short crack data of the type shown in Fig 6 must be coupled with an analysis of the probability of linking which depends on the microcrack population currently being characterized. In the latter case, the modeling must take into account the dependence of microcrack density on cycles, porosity level, and strain amplitude. The final stage, growth of long cracks, should obey crack growth laws such as a form of the Paris relationship but with modifications for roughness-induced crack closure in particular. Taken as a whole,

this analysis should result in a constitutive equation capable of predicting the influence of porosity on low cycle fatigue. In-put variables will include the shape, scale, and volume fraction of porosity as well as the cyclic stress-strain response of the matrix material.

3. Processing and Properties of Copper-Niobium Microcomposites (with Kevin Zeik, Ph.D. candidate and Dr. Iver Anderson, Ames Laboratory)

The operating conditions of certain advanced structural systems, such as those encountered by the hypersonic space plane, impose a a new set of very stringent requirements on the next generation of materials. In particular, the presence of sharp, cyclic thermal transients in structural components operating at high temperatures in the presence of hydrogen (such as those encountered by the engine components of the aforementioned aircraft) require not only high temperature strength, thermal stability, and resistance to environmental embrittlement but also a high degree of thermal conductivity. Conventional high conductivity alloys which depend on strain hardening or precipitation hardening simply do not exhibit the required thermal stability. Therefore a new alloy, one which has both the high temperature stability and the required electrical and thermal conductivities, must be considered. A candidate material for such an application is a copper-niobium microcomposite.

The purpose of this study is to develop and subsequently investigate the high temperature microstructural stability, deformation and fracture behavior of a copper-based microcomposite formed from rapidly solidified, ultrafine powders. The alloys considered are characterized by discontinuous Nb-rich particles embedded in a Cu-rich matrix. Their high-temperature stability relies on the mutual insolubility of the copper and niobium phases. High-pressure gas atomization will be used to produce the ultrafine ($<1\mu m$) rapidly solidified powders. A primary goal of the program is to process the powders into bulk form while maintaining a microstructure comprised of a continuous copper matrix and discontinuous niobium-rich particles. The particles must be sufficiently small and closely

spaced such that, at the volume fractions employed (~20%), a large strengthening increment is obtained, and retained, to temperatures up to 750°C.

The preliminary efforts have been directed at modifying the high pressure gas atomizer at the Naval Research Laboratory in Washington, D.C.. The atomizer crucible and pour tube assembly has been successfully fabricated from Cermotherm 2040, a molybdenum-zirconia composite which has permitted Cu-Nb alloys to be melted at temperatures exceeding 1900°C without any significant degredation either to the melt itself or the crucible/pour tube assembly after a short time (18 min) exposure. This, in conjunction with modifications to the temperature sensing equipment (the installation of high temperature Pt-Pt/10%Rh thermocouples) has allowed the atomizer to be safely used at temperatures far above any which had been previously considered.

Initial attempts to produce ultrafine powders of copper-15% niobium were not successful. Upon examination of the atomizer, it was determined that the Cu-Nb melt had frozen in the pour tube before exiting into the gas stream for atomization. Although the melt had been super heated to approximately 200°C above the calculated melting point of the alloy (1700°C), the heat losses from conduction by the pour tube caused solidification. Through careful consideration, the failure has been attributed to a lack of preheat in the pour tube assembly (the tube assembly was at ambient temperature). The solution now under investigation is based on of fitting a preheater into the pour tube prior to the atomization experiment. This preheater would raise the pour tube to a temperature exceeding 1200°C; it is postulated that under these new processing conditions the copper-niobium melt would contain sufficient superheat to remain liquid until contact with the gas stream. Requirements for such a heater include that its size be compatible with the existing pour tube assembly, that the heater sheath not react with the assembly, and that it can provide sufficient power as to raise the pour tube to a temperature exceeding 1200°C. These considerations are now under investigation and the evidence gathered indicates that

the heater being evaluated (manufactured by Chromalox Corporation, Pittsburgh, PA.), should prove successful.

The next atomization experiment is scheduled for May 1988. This experiment will also be conducted at the Naval Research Laboratory, Washington D. C., and will include the above modifications to the atomizer pour tube assembly. It will again involve the atomization of ultrafine Cu-15%Nb powders. After the successful production of the powder, several techniques will then be explored to consolidate them to a fully dense bulk form, including press and sinter and hot isostatic pressing. Microstructural characterization, stability, and property evaluations will be performed subsequently.

ACKNOWLEDGMENT

This research was supported by the Office of Naval Research through Contract No. N00014-86-K-0381.

REFERENCES

1. A. R. Cox, J. B. Moore, and E. C. Van Reuth, in Superalloys: Metallurgy and Manufacture, Claitor's Press, Baton Rouge, LA, p. 45, 1976.
2. M. Cohen, B. H. Kear, and R. Mehrabian, in Proc. of 2nd Int. Conf. on Rapid Solidification, Claitor's Press, Baton Rouge, LA, p. 1, 1980.
3. N. J. Grant, J. of Metals, 35, 20 (1983).
4. S.M.L. Sastry, T. C. Peng, and J. E. O'Neal, in Proc. Int. Powder Met. Conf., Toronto, June, 1984.
5. R. Haynes, The Mechanical Behavior of Sintered Alloys, Freund Publishing House, London, 1981.
6. E. A. Dubensky and D. A. Koss, in Aluminum Alloys, Their Physical and Mechanical Properties, Vol. II, Engineering Materials Advisory Services, U.K., p. 999, 1986.
7. E. A. Dubensky and D. A. Koss, Metall. Trans, 18A, 1887 (1987).
8. P. E. Magnusen, D. A. Koss, and E. M. Dubensky, Acta Met. (in print).
9. P. E. Magnusen, D. J. Srolovitz, and D. A. Koss, submitted for publication; see also ONR Technical Report No. 7, ONR Contract No. N00014-86-K-0381, 1987.
10. F. A. McClintock, J. of Appl. Mech., 35, 363 (1968).
11. A. Needleman, J. of Appl. Mech., 39, 964 (1962).
12. M. Nagumo. Acta Metall., 21, 1661 (1973).
13. B. I. Elelson, Trans. ASM, 56, 82 (1963).
14. S. I. Oh and S. Kobayashi, Tech. Rep. AFML-TR-76-61 (1976).
15. P. F. Thomason, Acta Metall., 29, 763 (1981).
16. V. Tvergaard, Int. J. Frac., 17, 389 (1981).
17. V. Tvergaard, Int. J. Frac., 18, 237 (1982).
18. P. F. Thomason, Acta Metall., 33, 1079 and 1087 (1985).
19. L. M. Brown and J. D. Embury, in Proc. 3rd Int. Conf. Strength of Metals and Alloys, p. 164, 1973.
20. R. A. Tait and D.M.R. Taplin, Scripta Met., 13, 77 (1979).
21. G. LeRoy, J. D. Embury, G. Edward and M. F. Ashby, Acta Metall., 29, 1509 (1981).

22. H. Yamamoto, Int. J. Frac., 14, 347 (1978).

23. M. Sage, J. Pan, and A. Needleman, Int. J. Frac., 19, 163 (1982).

24. P. E. Magnusen, unpublished research, 1987.

25. N. E. Dowling, in Cyclic Stress-Strain and Plastic Deformation Aspects of Fatigue Crack Growth, ASTM STP 637, (ASTM, Philadelphis) p. 97 (1977).

26. J. L. Robinson and C. L. Beevers, Metals Science Journal, 7, 153 (1973).

27. R. A. Das Gupta and R. A. Queeney, Int. J. Fatigue, 2, 113 (1980).

28. P. DiMascio and R. A. Queeney, Int. J. Powder Metal., 19, 127 (1983).

29. R. H. Rausket, R. D. Pendse, and R. O. Ritchie, Acta Metall., 35, 2227 (1987).

30. N. S. Iyer and N. E. Dowling, in Small Fatigue Cracks, (TMS-AIME), p. 213, 1986.

31. T. Seeger and P. Hueler, J. Testing and Evaluation 8, 199 (1980).

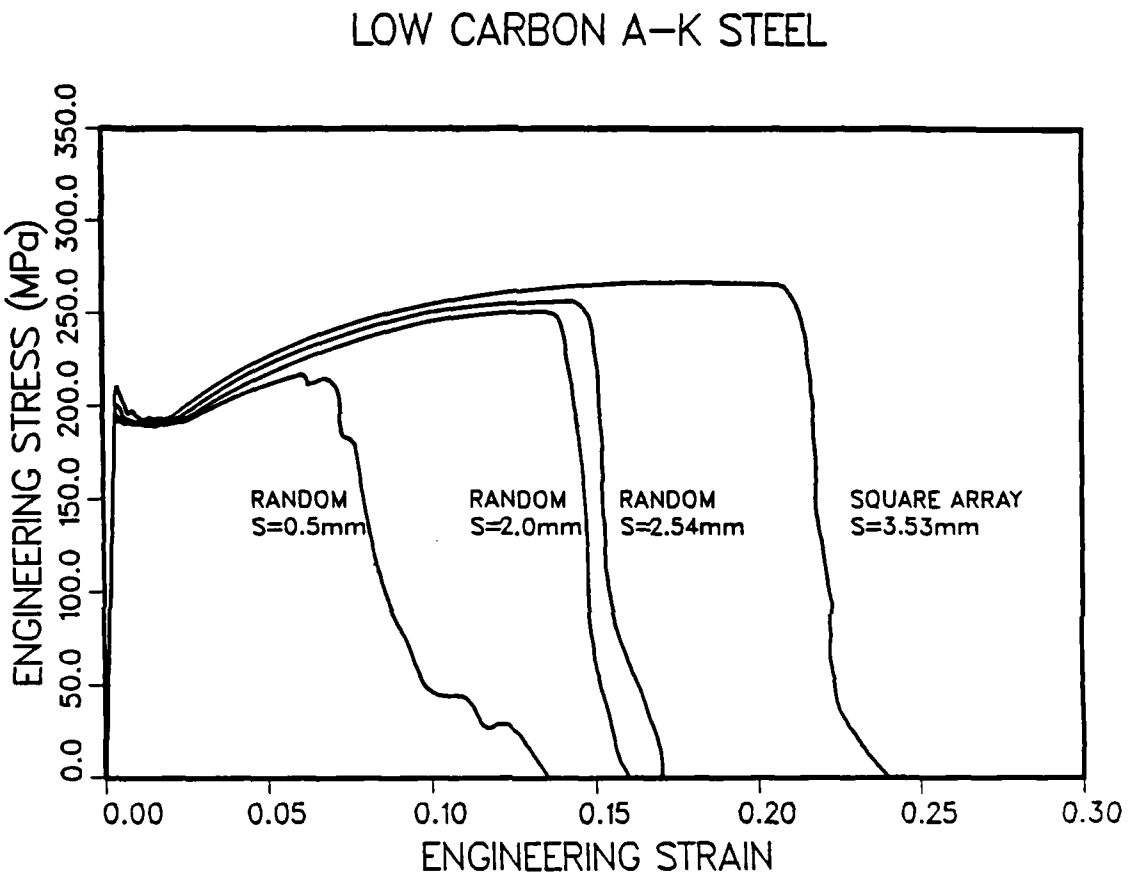

Figure 1. Engineering stress-strain behavior as a function of the hole array for low carbon steel sheet.

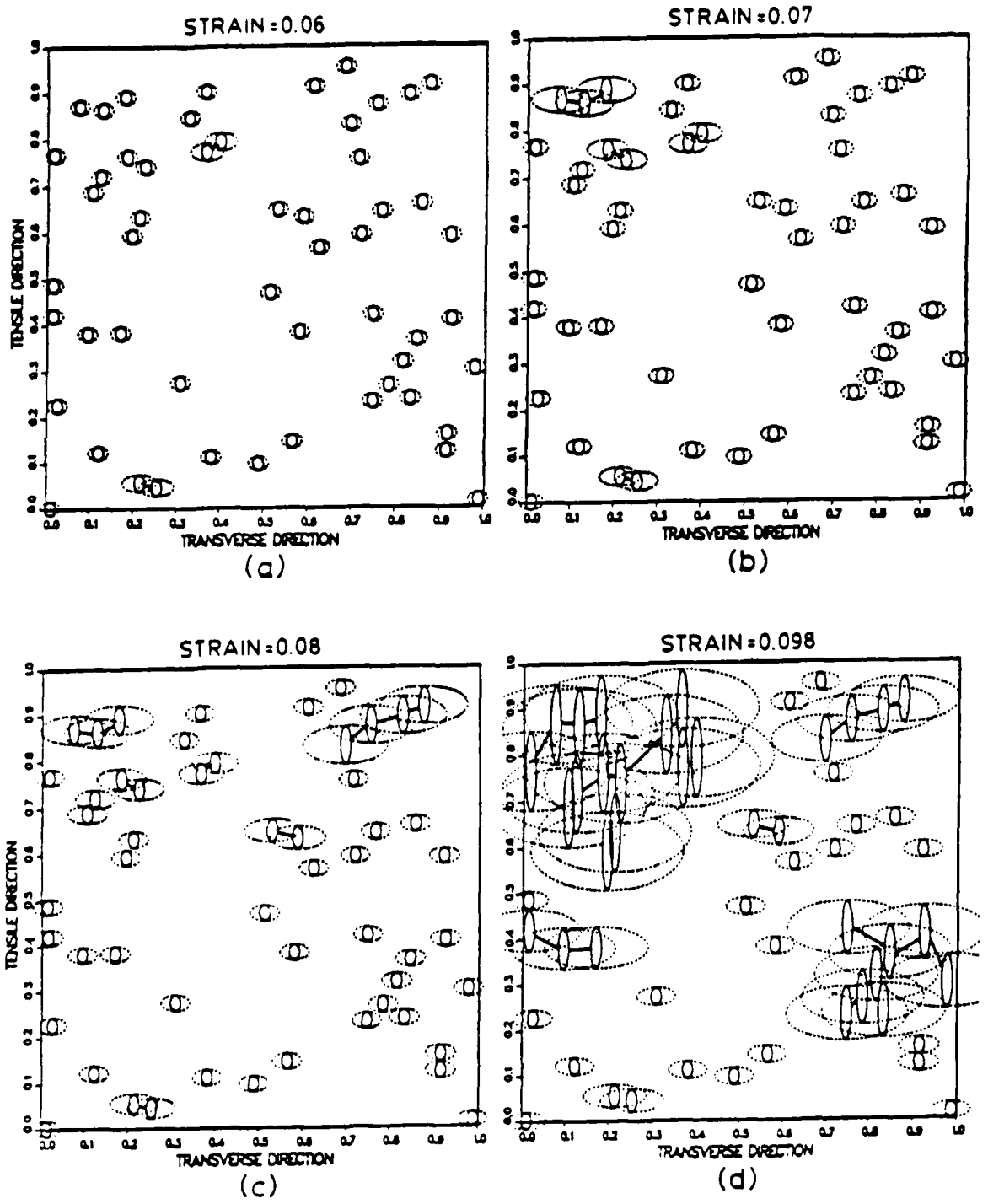

Figure 2. The simulated sequence of fracture events in 1100 aluminum with 0.05 area fraction of 1.2mm holes and a minimum hole spacing of 0.5mm. The macroscopic tensile strains are (a) $\varepsilon_1 = 0.06$, (b) $\varepsilon_1 = 0.07$, (c) $\varepsilon_1 = 0.08$, and (d) $\varepsilon_1 = 0.098$.

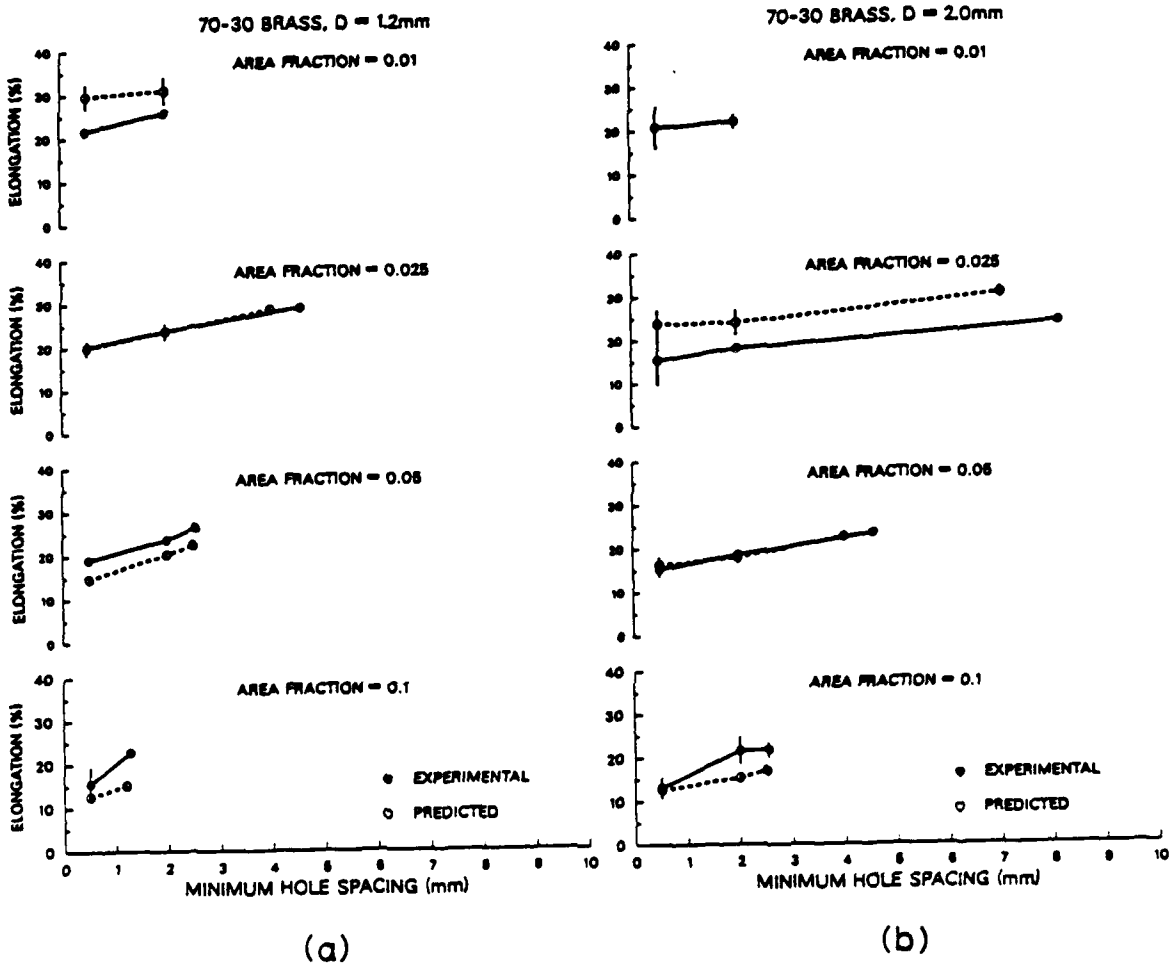

Figure 3. The dependence of the elongation to failure of 70-30 brass on the minimum hole spacing from both the experimental model and diameters of (a) d = 1.2mm and (b) d = 2.0mm.

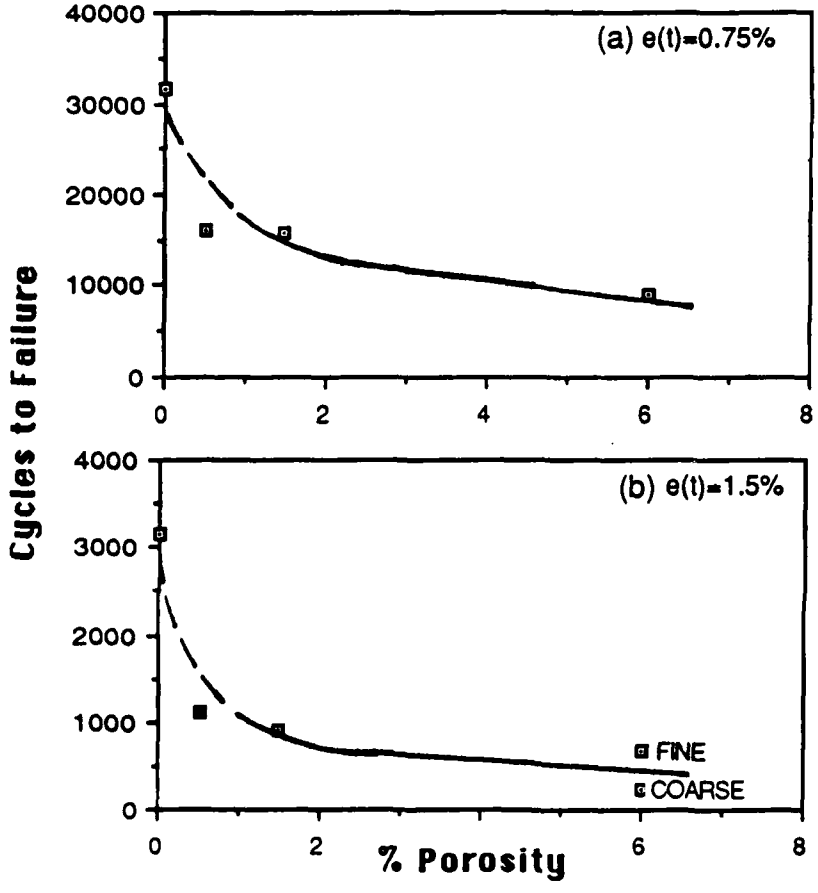

Figure 4. The number of cycles to failure as a function of porosity condition for fully reversed total strain amplitude tests at (a) 0.75% and (b) 1.5% strain.

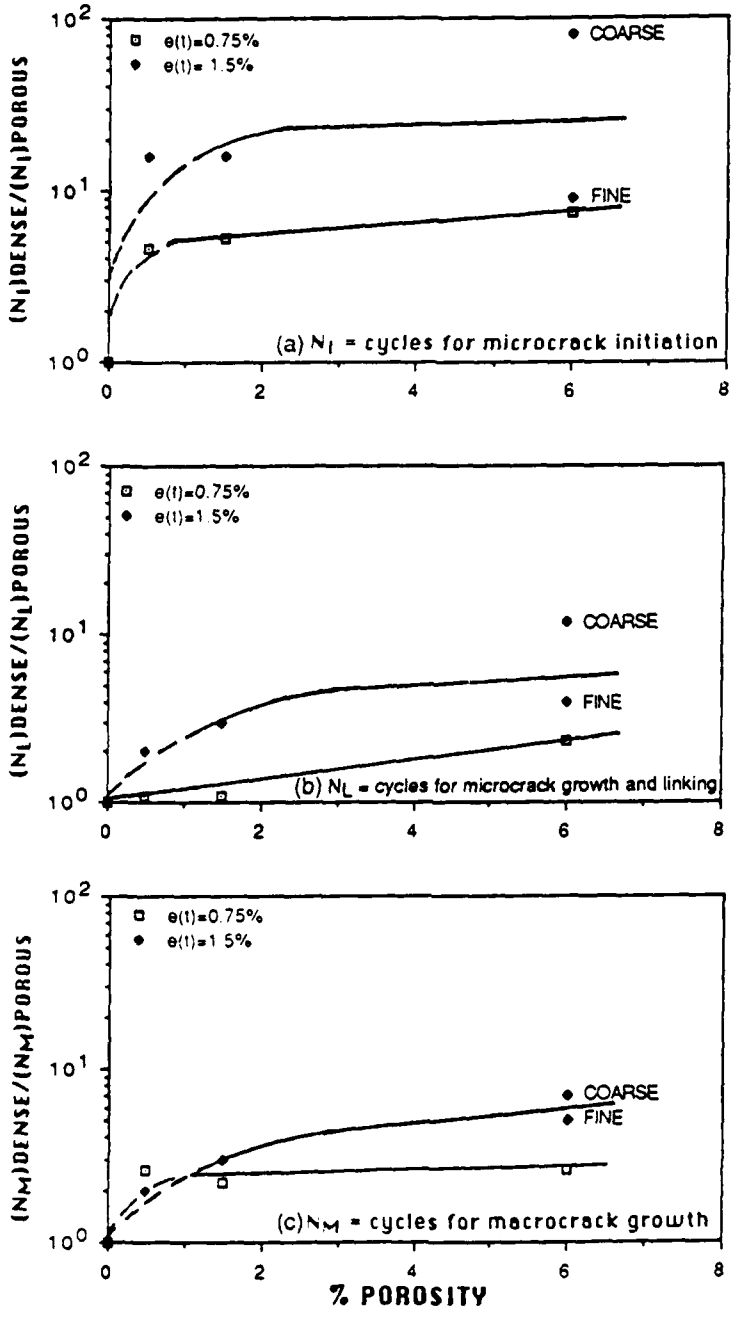

Figure 5. The number of cycles for each of the LCF failure stages of the fully dense material normalized to the individual failure stages of the porous titanium. The ratios indicate the effect that porosity has on accelerating each of the stages of fatigue failure when compared to the fully dense titanium.

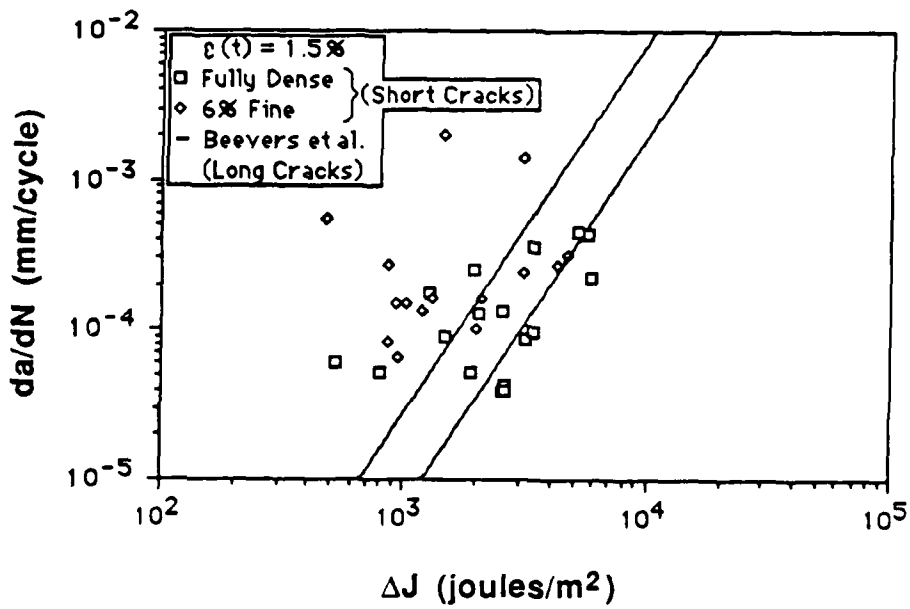

Figure 6. Short crack growth rates of the fully dense and 6% fine porosity titanium tested at a total strain amplitude of 1.5%. The growth rates are plotted against the J integral. The solid lines indicate large crack growth data regime extrapolated from work on fully dense titanium by Beevers et al..[26]

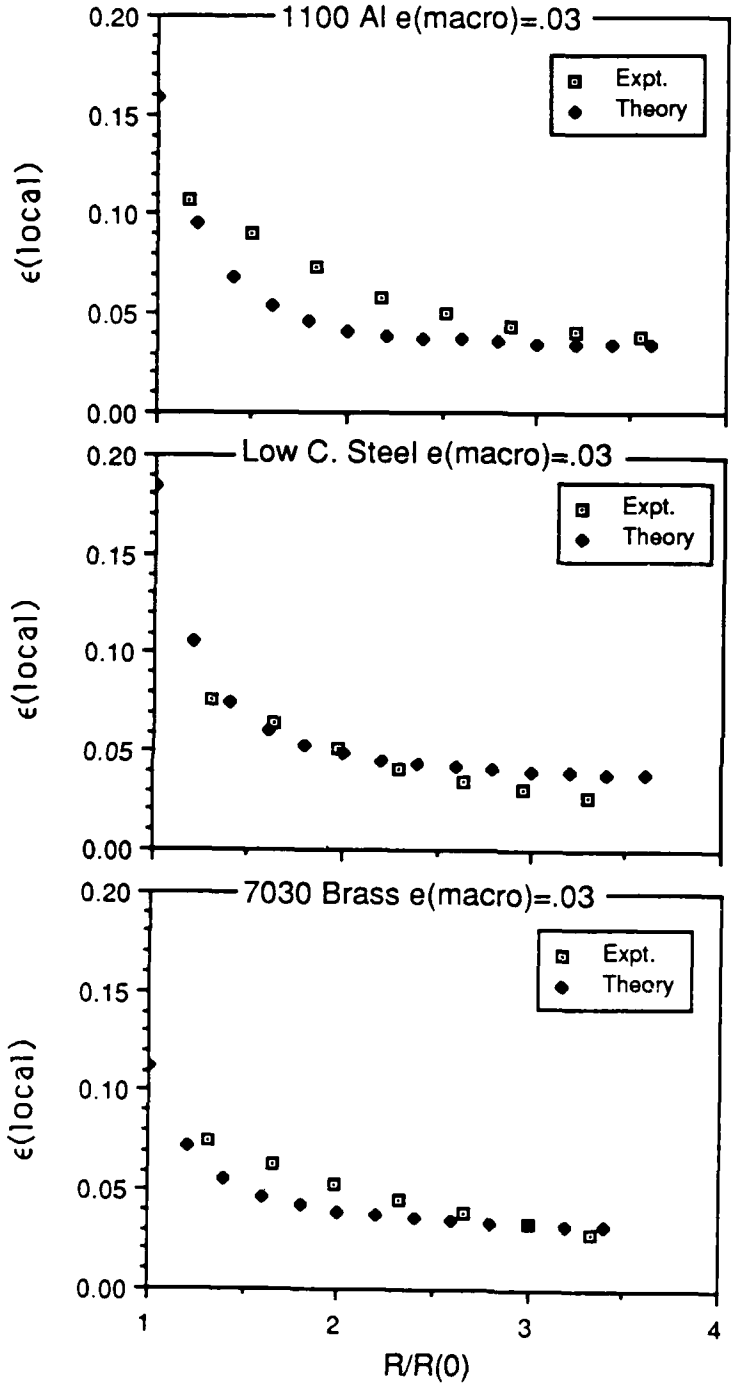

Figure 7. Theoretical and experimental plastic strain profiles in the vicinity of a through thickness hole. The strain profiles are taken from the plane normal to the fatigue axis. The strain profiles are plotted against the distance R away from the hole normalized to the hole radius R(0) for: (a) 70-30 α-brass, (b) a low carbon steel, and (c) 1100 Aluminum sheets deformed in uniaxial tension to macroscopic strain levels of 8%.

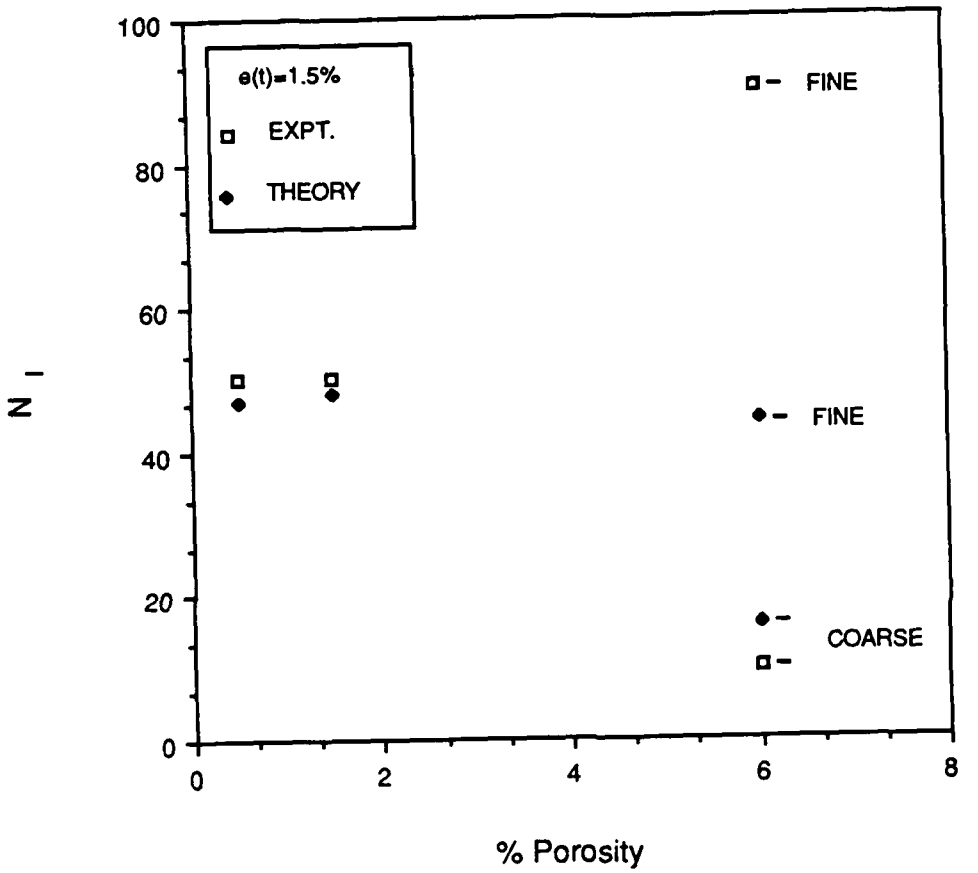

Figure 8. A comparison of the predicted and experimentally determined number of cycles to initiate a crack N_I as a function of porosity content. Specimens are cycled at a total strain amplitude of 1.5%.

END
DATE
FILMED
7-88
DTIC